



Numerical Analysis of Double Diffusive Laminar Natural Convection in a Right Angle Triangular Solar Collector

Jasim M. Mahdi*

Ali M. Rasham**

Thamir H. Ali***

*,**Department of Energy Engineering / College of Engineering / University of Baghdad

*** Department of Manufacturing Engineering / Al-Khwarizmi College of Engineering / University of Baghdad

*E-mail: jasim_ned@yahoo.com

**E-mail: ali_mohsen7788@yahoo.com

***E-mail: thamir.2008@yahoo.com

(Received 6 December 2012; accepted 12 January 2014)

Abstract

A numerical study of the double-diffusive laminar natural convection in a right triangular solar collector has been investigated in present work. The base (absorber) and glass cover of the collector are isothermal and isoconcentration surfaces, while the vertical wall is considered adiabatic and impermeable. Both aiding and opposing buoyancy forces have been studied. Governing equations in vorticity-stream function form are discretized via finite-difference method and are solved numerically by iterative successive under relaxation (SUR) technique. Computer code for MATLAB software has been developed and written to solve mathematical model. Results in the form of streamlines, isotherms, isoconcentration, average Nusselt, and average Sherwood number, are presented for wide range of the buoyancy ratio ($-1 \leq N \leq 5$), angle of inclined glass cover with horizontal coordinate ($30^\circ \leq \theta \leq 60^\circ$), Lewis number ($Le = 2$), thermal Rayleigh number ($10^3 \leq Ra_T \leq 10^5$), and Prandtl number ($Pr = 0.71$). The results show that above parameters have strong influences on the patterns of streamline, isotherms, isoconcentration, average Nusselt number and average Sherwood number. Results show that a decrease in the angle of inclined glass cover with horizontal coordinate (θ) leads to increase average Nusselt number and average Sherwood number. For ($N > 0$), both average Nusselt number and average Sherwood number increase with increasing of buoyancy ratio and Rayleigh number. By contrast for ($N < 0$) these values decreases. Also, increasing of the buoyancy ratio for positive ($N > 0$), at the same Rayleigh number enhance the heat and mass transfer rate. A comparison is made with the previous numerical results and it found to be reveal a good agreement.

Keywords: double diffusion, heat and mass transfer, laminar natural convection, solar collector.

1. Introduction

A double diffusive Natural convection in solar collector of various forms occupies a large portion of heat transfer literature. A few numbers of studies have considered the triangular geometry, which is encountered in several practical engineering applications, such as water desalination plants. Hitesh N Panchal, etc., [1] studied effect of varying glass cover thickness on performance of solar still: in a winter climate conditions. Six-month-study showed that, lower glass cover thickness increases the distillate water

output, water temperature, evaporative heat transfer coefficient, convective heat transfer coefficient as well as efficiency of solar still. Hiroshi Tanaka, [2] investigated a theoretical analysis of basin type solar still with flat plate external reflector. Narjes Setoodeh, etc., [3] reviewed the Modeling and determination of heat transfer coefficient in a basin solar still using CFD. The simulation results were compared with the available experimental data of basin solar still. M.M. Rahman, etc. [4] presented a double diffusive natural convection in triangular solar collector. The study deals with natural convection

flow resulting from the combined buoyancy effects of thermal and mass diffusion inside a triangular shaped solar collector. Mohamed A. Teamah, [5] researched numerically a Double-diffusive convective flow in a rectangular enclosure with the upper and lower surfaces being insulated and impermeable. Constant temperatures and concentration are imposed along the left and right walls of the enclosure. In addition, a uniform magnetic field is applied in a horizontal direction. Laminar regime is considered under steady state condition. Ching-Yang Cheng, [6] employed the double diffusive natural convection near an inclined wavy surface in a fluid saturated porous medium with constant wall temperature and concentration. Effects of angle of inclination, Lewis number, buoyancy ratio, and wavy geometry on the heat and mass transfer characteristics are studied. The same author [7] analyzed the coupled heat and mass transfer by natural convection near a vertical wavy surface in a non-Newtonian fluid saturated porous medium with thermal and mass stratification. The surface of the vertical wavy plate is kept at constant wall temperature and concentration. The total heat transfer rate and the total mass transfer rate of vertical wavy surfaces are higher than those of the corresponding smooth surfaces. Yasin Varol, etc., [8] performed that steady-state free convection heat transfer in a right-angle triangular enclosure, whose vertical wall insulated and inclined and bottom walls are differentially heated. The governing equations are obtained using Darcy model. The governing equations were solved by finite difference method and solution of algebraic equations was made via Successive under Relaxation method. Ali J. Chamkha, etc., [9] scrutinized hydromagnetic double diffusive convection in a rectangular enclosure with opposing temperature and concentration gradients. Constant temperatures and concentrations are imposed along the left and right walls of the enclosure and a uniform magnetic field is applied in the x-direction. the thermal and compositional buoyancy forces are assumed to be opposite. E. Fuad Kent, etc., [10] examined numerically natural convection in nonrectangular enclosures. Streamlines and isotherms are presented for different triangular enclosures with different boundary conditions and Rayleigh numbers. Mean Nusselt numbers on hot walls are also calculated in order to make comparisons between different cases. E. F. Kent, [11] explored the numerical analysis of laminar natural convection in isosceles triangular enclosures for two different thermal boundary conditions. In case 1, the base is heated

and the two inclined walls are symmetrically cooled, and in case 2, the base is cooled and the two top inclined walls are symmetrically heated. Base angles varying from 15 to 75° have been used for different Rayleigh numbers ranging from 10³ to 10⁵. Yoshio Masuda, etc., [12] showed analytically and numerically a Double-diffusive natural convection in a rectangular fluid-saturated porous Medium. The analysis reveals that there is a range of buoyancy ratios N in which one obtains two types of solutions or oscillating convection. In the case of 0.4 < N < 1.0, there exist two analytical solutions when Rc = 100 and Le = 30. In that case, two solutions, temperature-dominated and concentration-dominated solutions, are calculated when the aspect ratio is small.

2. Mathematical Formulation

The schematic of the system under consideration is shown in Fig (1). The salty water on the bottom side (T_H) of the glazing enclosure is vaporized from the liquid-vapor interface. The vapor moves through the air and condenses at the cooled side walls (T_L). The vertical wall is assumed to be adiabatic and impermeable. The fluid is assumed to be incompressible, Newtonian, absorbing, viscous, and two dimensional at steady state conditions. According to the above assumptions, these equations can be written in dimensional form as

Continuity equation

$$u \frac{\partial u}{\partial x} + v \frac{\partial v}{\partial y} = 0 \quad \dots(1)$$

X- momentum equation

$$u \frac{\partial u}{\partial x} + v \frac{\partial u}{\partial y} = -\frac{1}{\rho} \frac{\partial p}{\partial x} + \nu \left(\frac{\partial^2 u}{\partial x^2} + \frac{\partial^2 u}{\partial y^2} \right) \quad \dots(2)$$

Y- momentum equation

$$u \frac{\partial v}{\partial x} + v \frac{\partial v}{\partial y} = -\frac{1}{\rho} \frac{\partial p}{\partial y} + \nu \left(\frac{\partial^2 v}{\partial x^2} + \frac{\partial^2 v}{\partial y^2} \right) + g\beta_T(T - T_c) + g\beta_c(c - c_c) \quad \dots(3)$$

Energy equation

$$u \frac{\partial T}{\partial x} + v \frac{\partial T}{\partial y} = \alpha \left(\frac{\partial^2 T}{\partial x^2} + \frac{\partial^2 T}{\partial y^2} \right) \quad \dots(4)$$

Concentration equation

$$u \frac{\partial c}{\partial x} + v \frac{\partial c}{\partial y} = D \left(\frac{\partial^2 c}{\partial x^2} + \frac{\partial^2 c}{\partial y^2} \right) \quad \dots(5)$$

The boussinesq approximation for the buoyancy term in the momentum equations have been employed,

$[\rho = \rho_{\infty} [1 - \beta_T(T - T_h) - \beta_C(c - c_h)]]$ [13]. The use of vorticity-stream function formulation can eliminate pressure gradient terms from momentum equations and simplify the solution procedure. With the stream function, the velocity components u and v and vorticity can be expressed as

$$u = (-\partial\psi/\partial y), v = (\partial\psi/\partial x) \text{ and } \omega = ((\partial u/\partial y) - (\partial v/\partial x))$$

And then introducing the following dimensionless groups for the governing equations, $(X, Y) = (x, y)/H, (U, V) = (u, v)/(\alpha/H), \Psi = \psi/\alpha, \Omega = \omega/(\alpha/H^2), \theta = (T - T_L)/(T_H - T_L)$

with $T_H > T_L$, And $C = (c - c_f)/(c_h - c_f)$ with $c_h > c_f$, the governing equations in terms of vorticity-stream function form become:

Stream function equation

$$\nabla^2 \Psi = -\Omega \quad \dots(6)$$

Vorticity equation

$$\nabla^2 \Omega = \frac{1}{Pr} \left[U \frac{\partial \Omega}{\partial X} + V \frac{\partial \Omega}{\partial Y} \right] - Ra \left(\frac{\partial \theta}{\partial X} + N \frac{\partial C}{\partial X} \right) \quad \dots(7)$$

Energy equation

$$\nabla^2 \theta = U \frac{\partial \theta}{\partial X} + V \frac{\partial \theta}{\partial Y} \quad \dots(8)$$

Concentration equation

$$\nabla^2 C = Le \left[U \frac{\partial C}{\partial X} + V \frac{\partial C}{\partial Y} \right] \quad \dots(9)$$

where U and V in equations (8-9) is as follow:

$$U = -\partial\Psi/\partial Y \text{ and } V = \partial\Psi/\partial X \quad \dots(10)$$

The dimensionless parameters appearing in equations (6 - 9) are the Prandtl number $Pr = \nu/\alpha$, $Le = \alpha/D$, the thermal Rayleigh number $Ra_T = g\beta_T(T_H - T_L)H^3/\alpha\nu$, the compositional Rayleigh number $Ra_C = g\beta_C(c_h - c_f)H^3/\alpha\nu$, and $N = \beta_C(c_h - c_f)/\beta_T(T_H - T_L)$. The appropriate boundary conditions in dimensionless form can be formulated as:

1. At the inclined surface (glass cover)

$$\Psi = 0, \frac{\partial^2 \Omega}{\partial n^2} = 0, \theta = C = 0$$

2. At the bottom surface (absorber)

$$\Psi = 0, \frac{\partial^2 \Omega}{\partial n^2} = 0, \theta = C = 1$$

3. At the vertical wall (adiabatic wall)

$$\Psi = 0, \frac{\partial^2 \Omega}{\partial n^2} = 0, \frac{\partial \theta}{\partial n} = 0, \frac{\partial C}{\partial n} = 0$$

The local heat transfer rates on the surface of heat source and local mass transfer on the surface of pollutant source are defined respectively as

$$Nu_x = -(\partial\theta/\partial Y)|_{Y=0} \text{ and } Sh_x = -(\partial C/\partial Y)|_{Y=0} \quad \dots(11)$$

The average Nusselt and Sherwood numbers represents the average heat and mass transfer rates on the surface of heat and pollutant sources [4], which are defined respectively as

$$Nu = - \int_0^1 (\partial\theta/\partial Y) dx \quad \dots(12)$$

$$Sh = - \int_0^1 (\partial C/\partial Y) dx \quad \dots(13)$$

3. Numerical Technique

The central difference scheme used to discretize the system of partial differential equations (6-10) via a finite difference method (FDM). Iterative under relaxation method (URM) used to solve the system of new algebraic equations to give approximate values of the dependent variables at a number of discrete points called (nodes) in the computational domain. the computational domain is subdividing in the X and Y directions with vertical and horizontal uniformly spaced grid lines to form these nodes. Fig (1) grid of 101×101 nodes is adopted typically in this study. However, to ensure the accuracy and validity of the numerical schemes, Five grid systems, 61×61 , 81×81 , 101×101 , 121×121 , and 151×151 are tested. Results show the average Nusselt number prediction for 101×101 grid points nearly correspond to that obtained from other grid points, the maximum relative error (% ϵ) obtained through the five grid systems is no more than 2% as shown in Table (1). The accuracy of the numerical code was assessed by applying it to a case studied by E. Fuad Kent, etc. [10], who considered a right

triangular enclosure similar to that being considered in this paper, the results in form of streamlines and isothermals contours for ($\theta = 45^\circ$), and different Rayleigh numbers (10^3 - 10^5) compared and excellent agreement was observed, Figures (2-3) respectively. The

convergence criteria employed to terminate the computations and reach the solution were reassigned as $(\Psi^\zeta - \Psi^{\zeta-1})/\Psi^\zeta \leq 10^{-6}$, $(\theta^\zeta - \theta^{\zeta-1})/\theta^\zeta \leq 10^{-6}$, $(C^\zeta - C^{\zeta-1})/C^\zeta \leq 10^{-6}$, and $(\Omega^\zeta - \Omega^{\zeta-1})/\Omega^\zeta \leq 10^{-6}$, the indices ζ and $\zeta - 1$ represent the current and previous iteration, respectively.

Table 1,
Grid Independence Study Results for Average Nusselt Number at (Br=0, $\alpha = 45^\circ$).

Size	61×61	81×81	101×101	121×121	151×151	% e
Ra = 10³	4.947	4.994	5.197	5.230	5.244	0.9
Ra = 10⁴	4.997	5.392	5.486	5.588	5.572	1.85
Ra = 10⁵	6.993	7.124	7.211	7.301	7.350	1.92

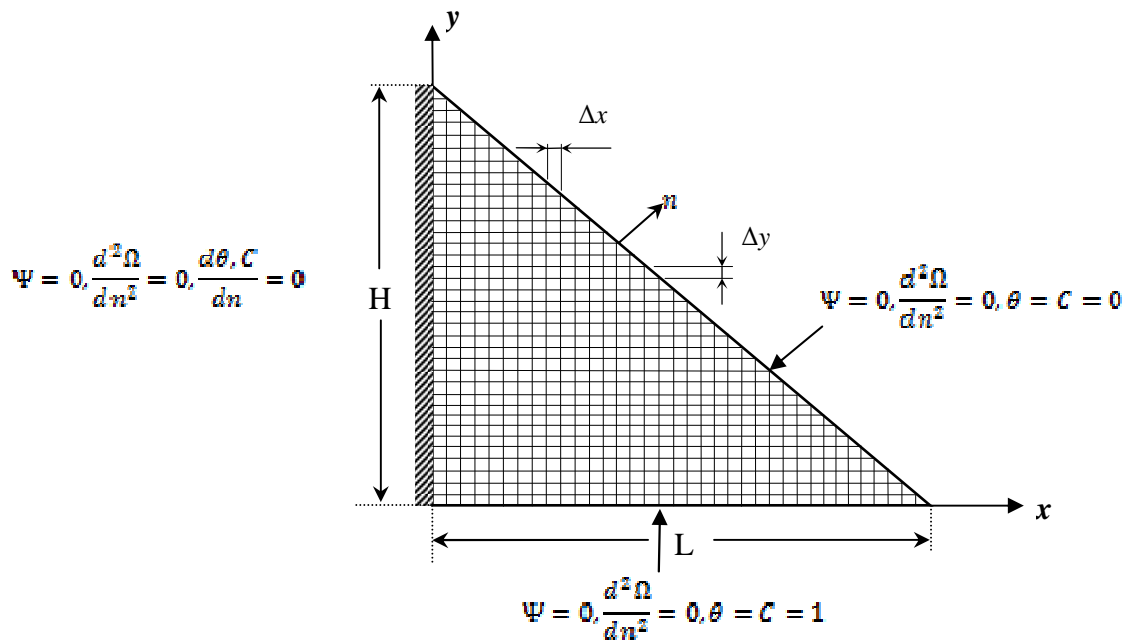


Fig.1 . A Schematic of the Geometry and Grid.

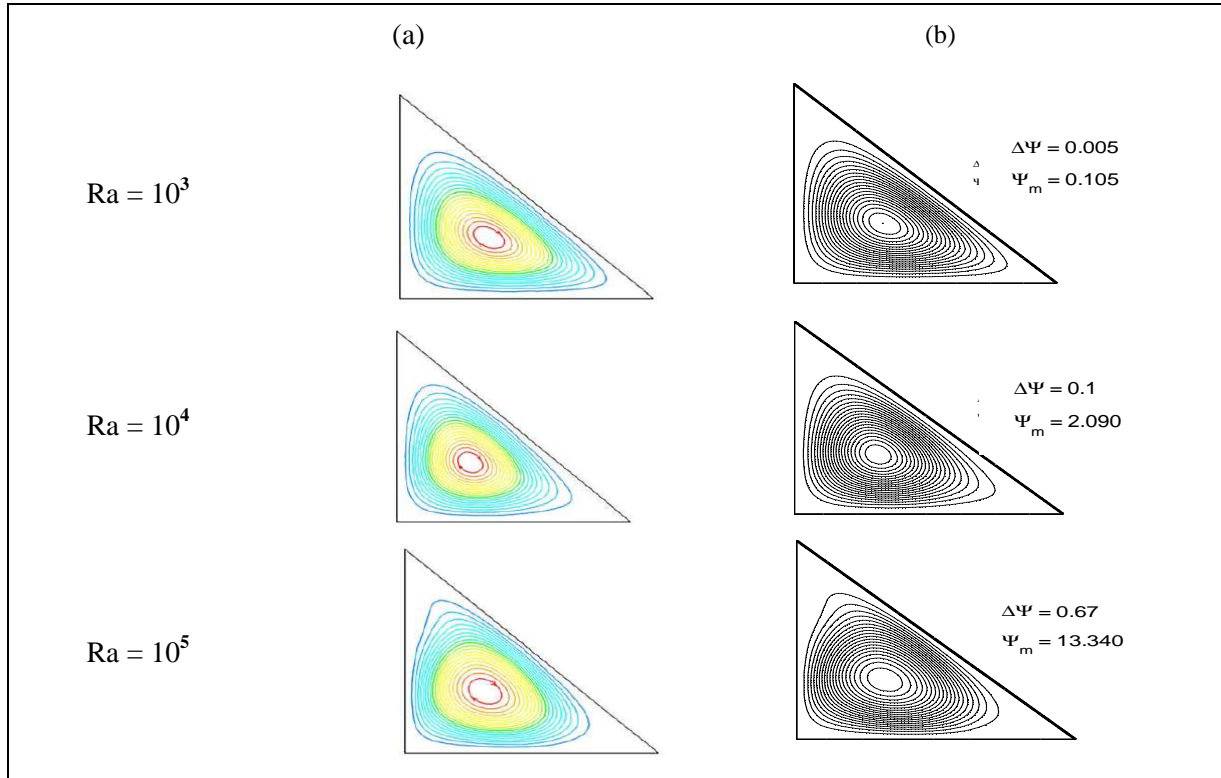


Fig. 2. Comparison of Streamlines Inside the Right Triangular Enclosure for Rayleigh Numbers $10^3, 10^4$ and 10^5 , Respectively Between (a) Kent (b) Present Study.

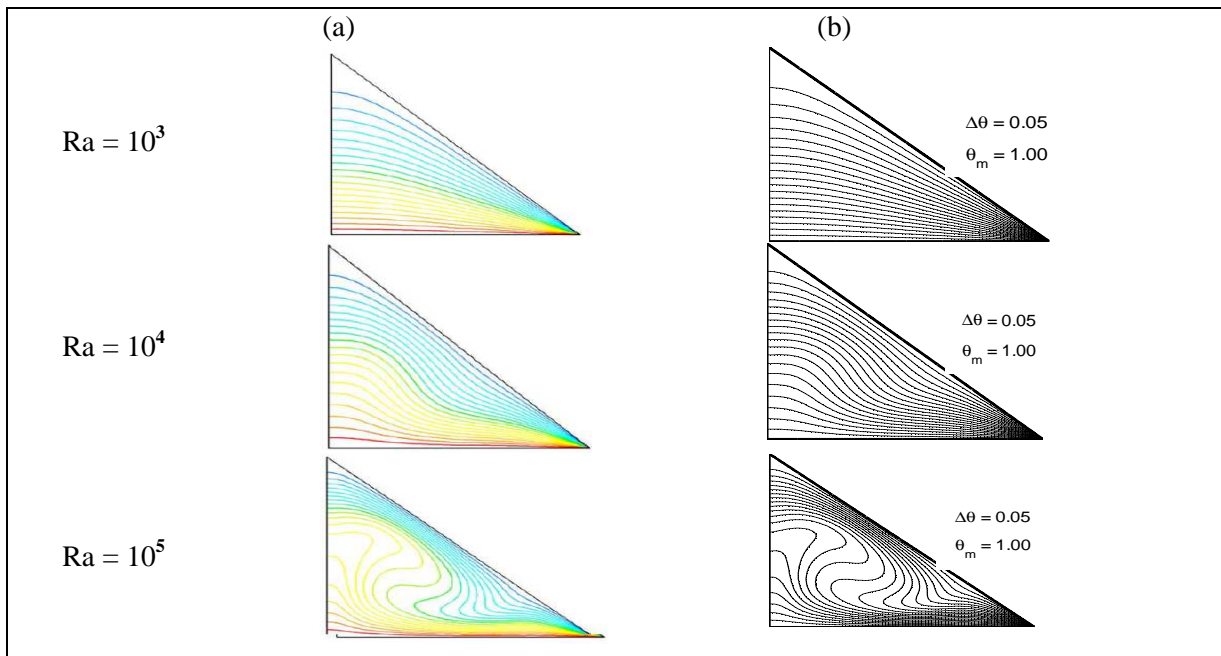


Fig. 3. Comparison of Isotherms Inside the Right Triangular Enclosure for Rayleigh Numbers $10^3, 10^4$ and 10^5 , Respectively Between (a) Kent (b) Present Study.

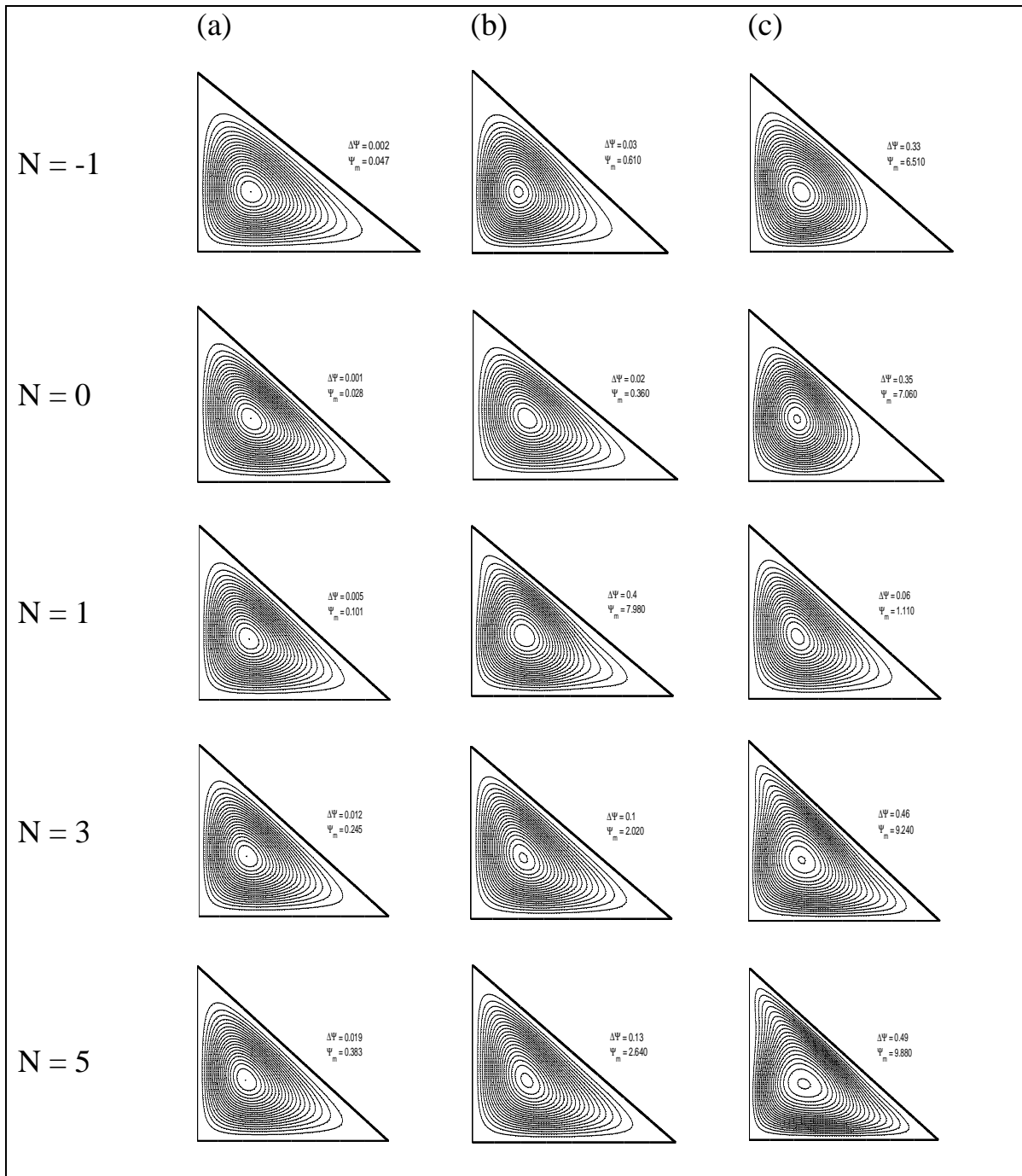


Fig. 4. Effect of Buoyancy Ratio on Streamlines at Le=2, and $\phi = 30^\circ$ for (a) Ra=10³, (b) Ra=10⁴, and (c) Ra=10⁵.

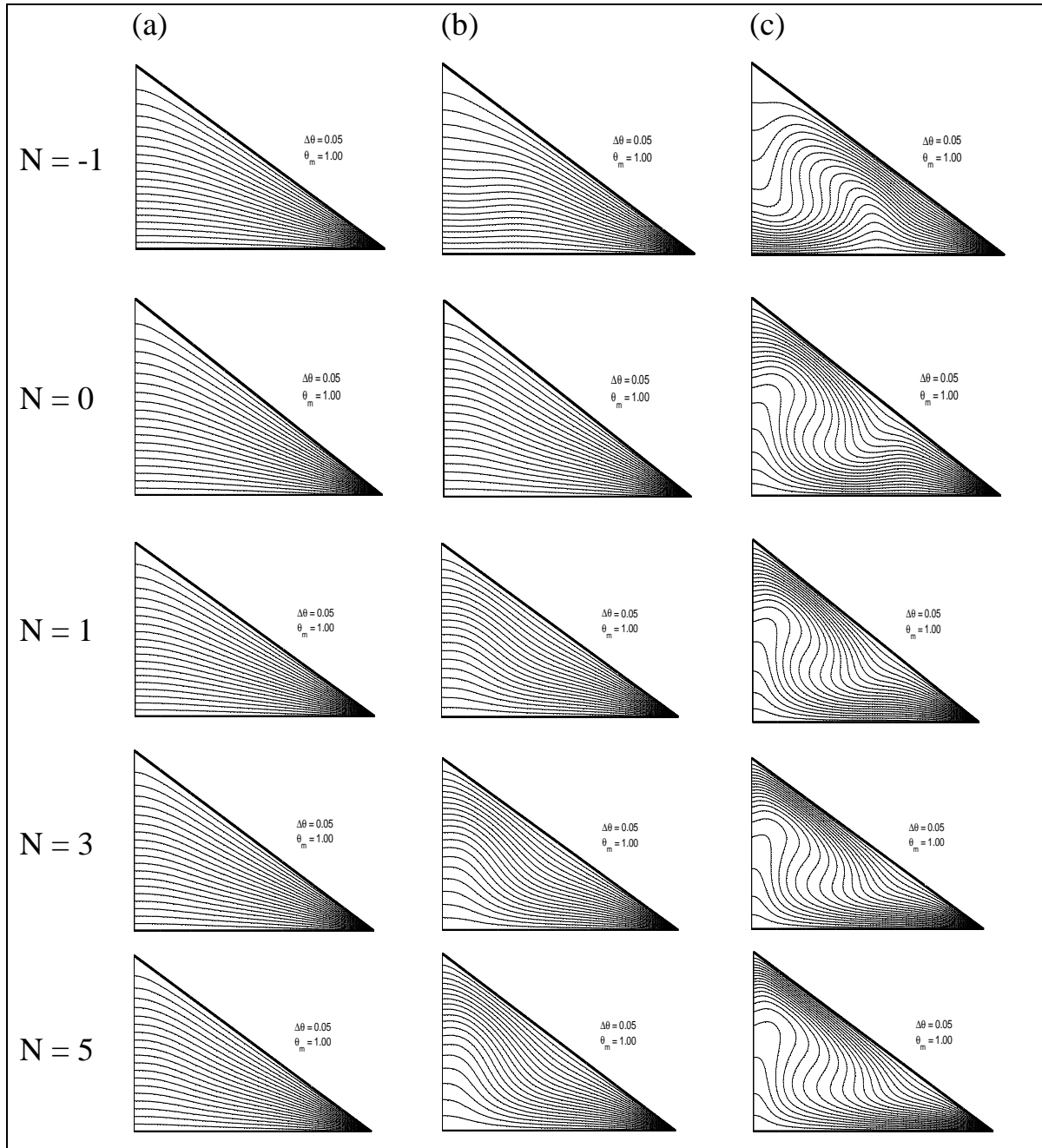


Fig. 5. Effect of Buoyancy Ratio on Isotherms $Le=2$, and $\phi = 30^\circ$ for (a) $Ra=10^3$, (b) $Ra=10^4$, and (c) $Ra=10^5$.

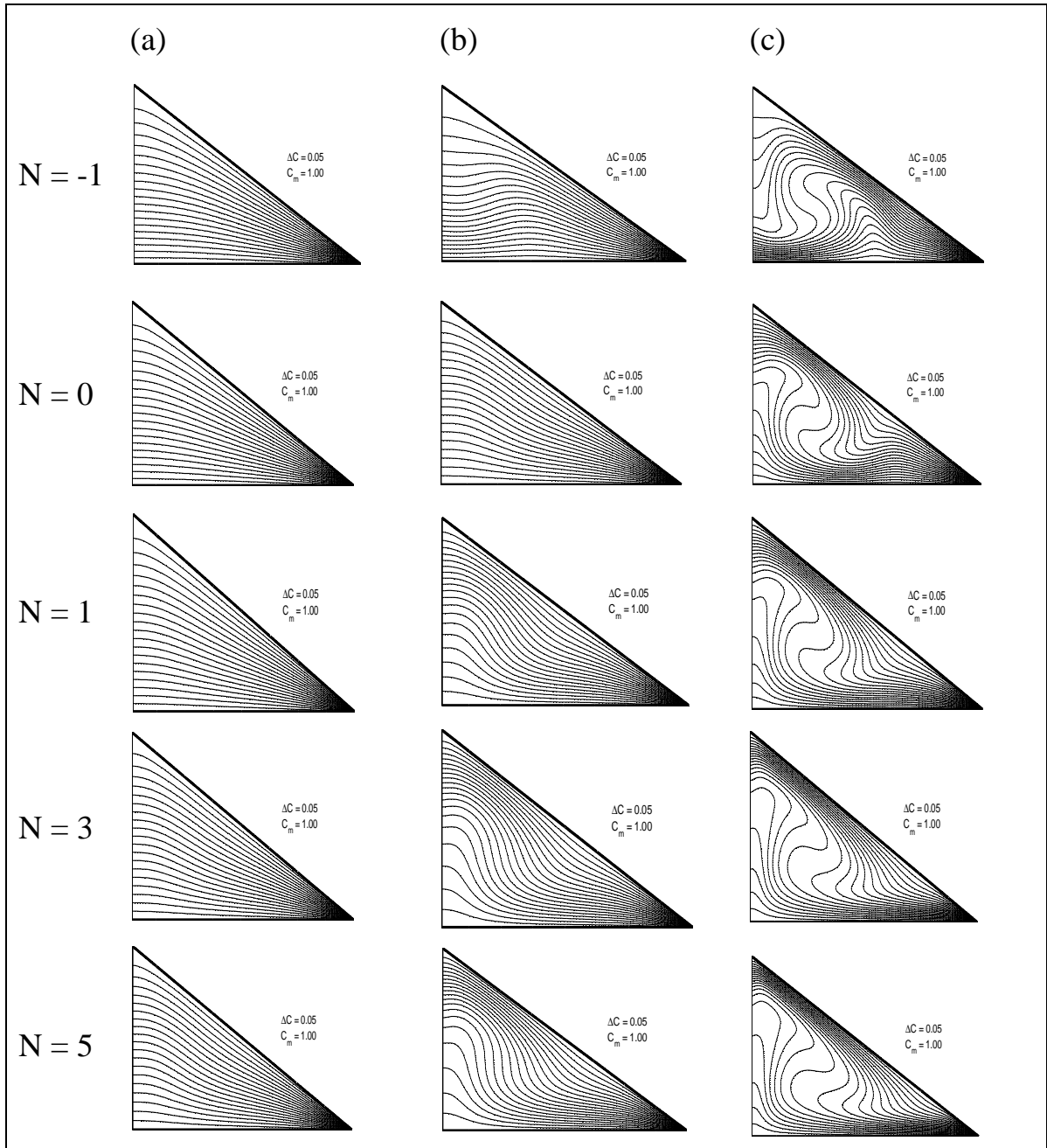


Fig. 6. Effect of Buoyancy ratio on Isoconcentration at $Le=2$, $\phi = 30^\circ$ for (a) $Ra=10^3$, (b) $Ra=10^4$, and (c) $Ra=10^5$.

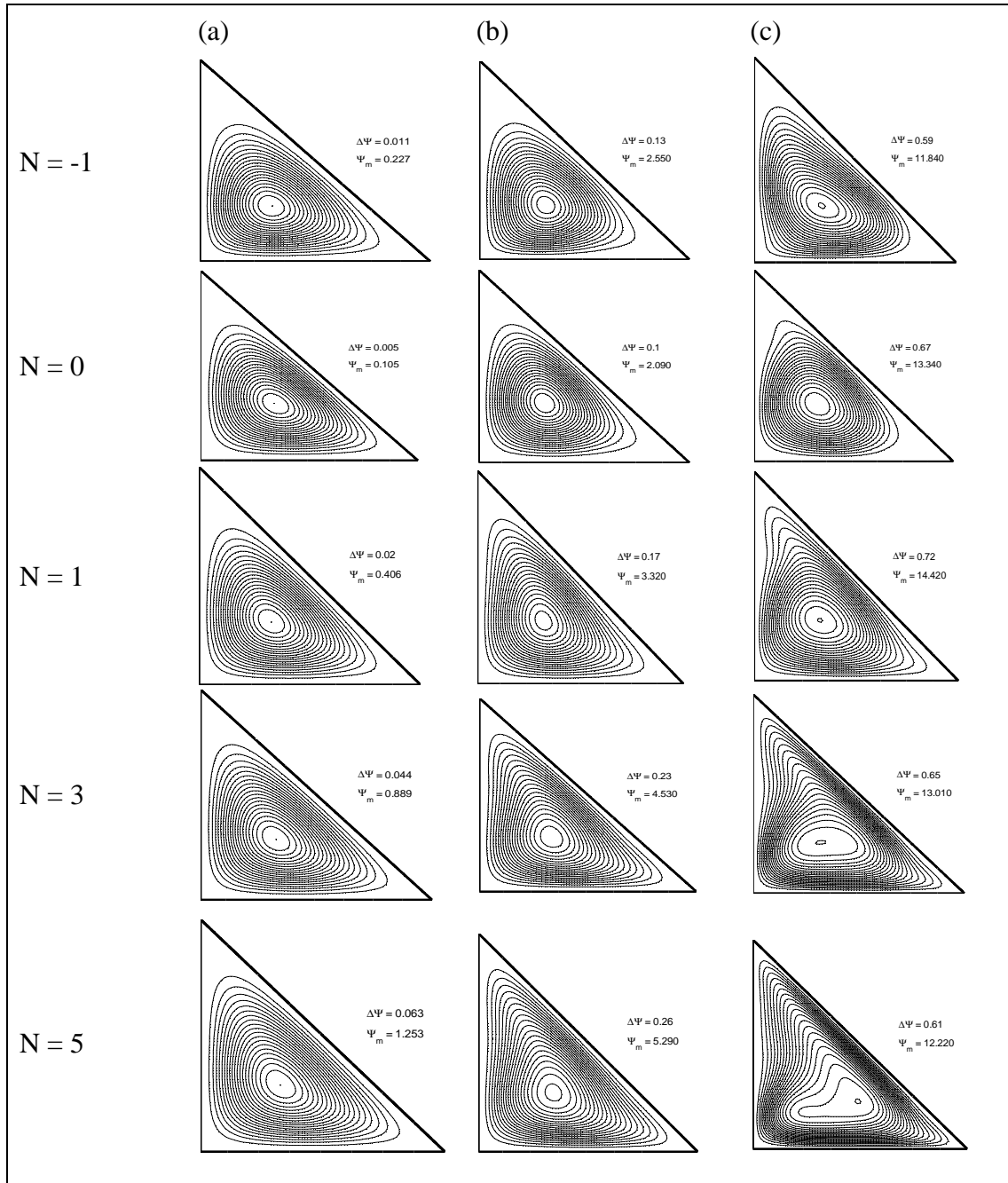


Fig. 7. Effect of Buoyancy Ratio on Streamlines at Le=2, and $\theta = 45^\circ$ for (a) Ra=10³, (b) Ra=10⁴, and (c) Ra=10⁵.

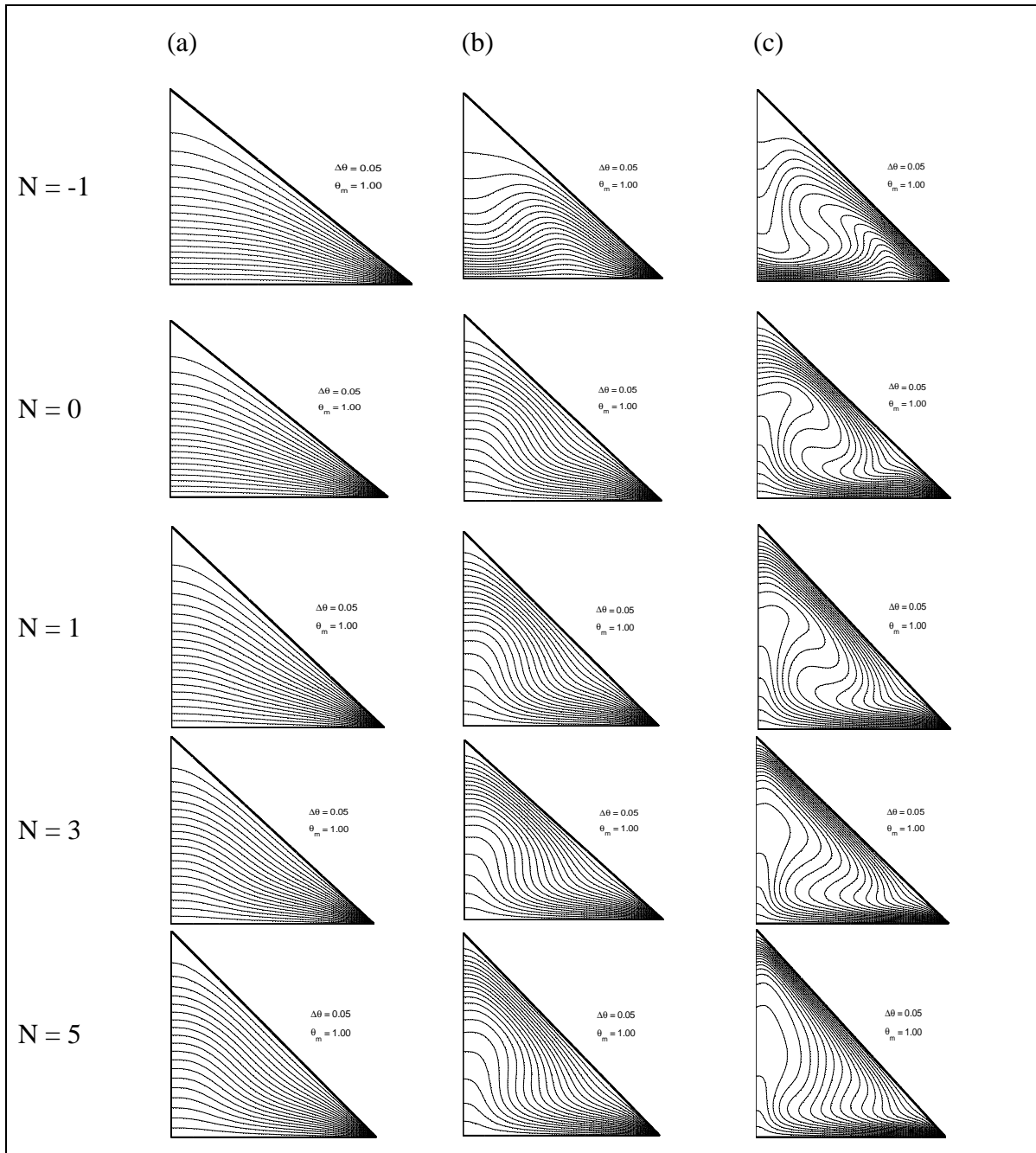


Fig. 8. Effect of Buoyancy Ratio on Isotherms at $Le=2$, and $\phi = 45^\circ$ for (a) $Ra=10^3$, (b) $Ra=10^4$, and (c) $Ra=10^5$.

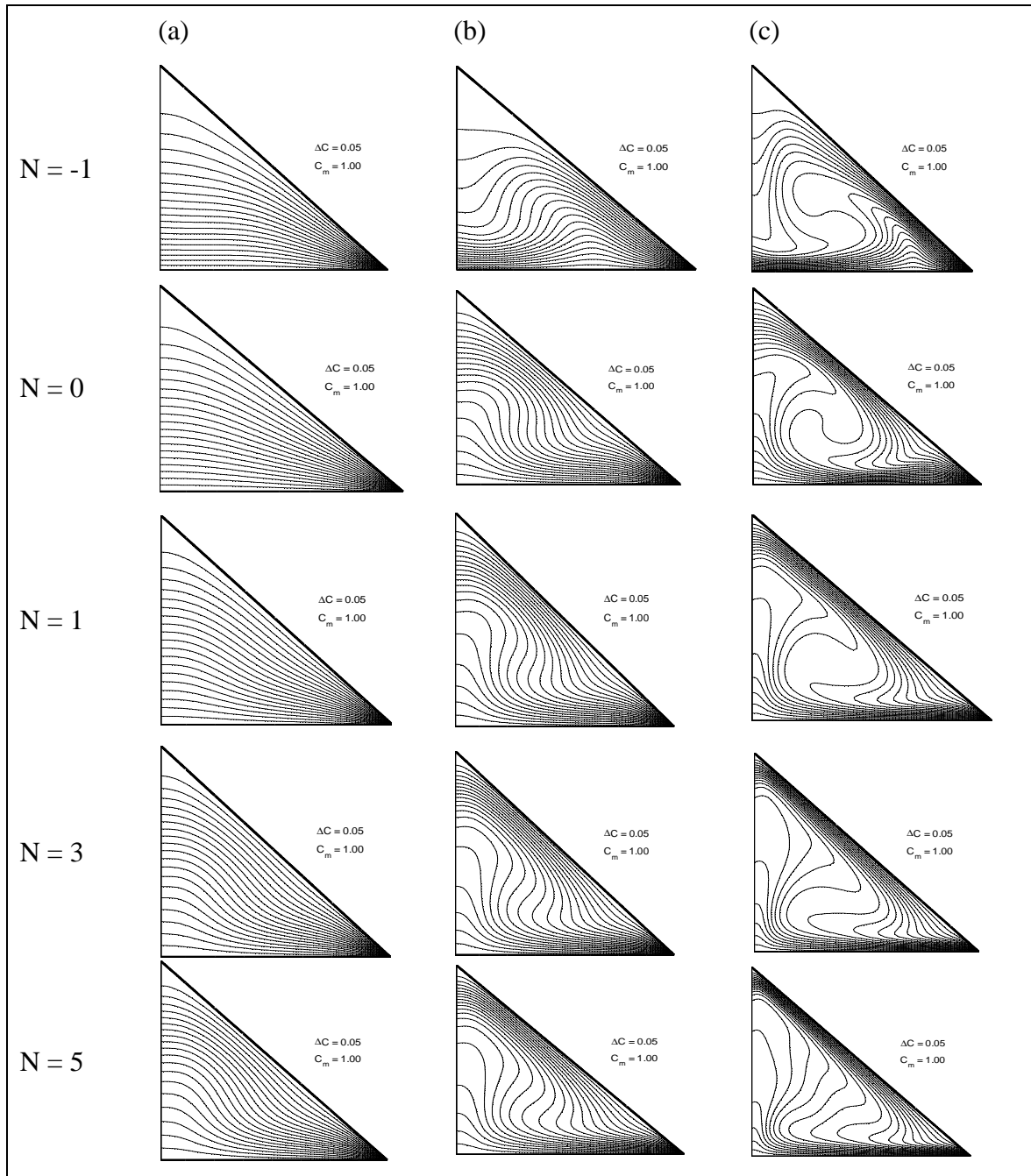


Fig. 9. Effect of Buoyancy Ratio on Isoconcentration at $Le=2$, and $\phi = 45^\circ$ for (a) $Ra=10^3$, (b) $Ra=10^4$, and (c) $Ra=10^5$.

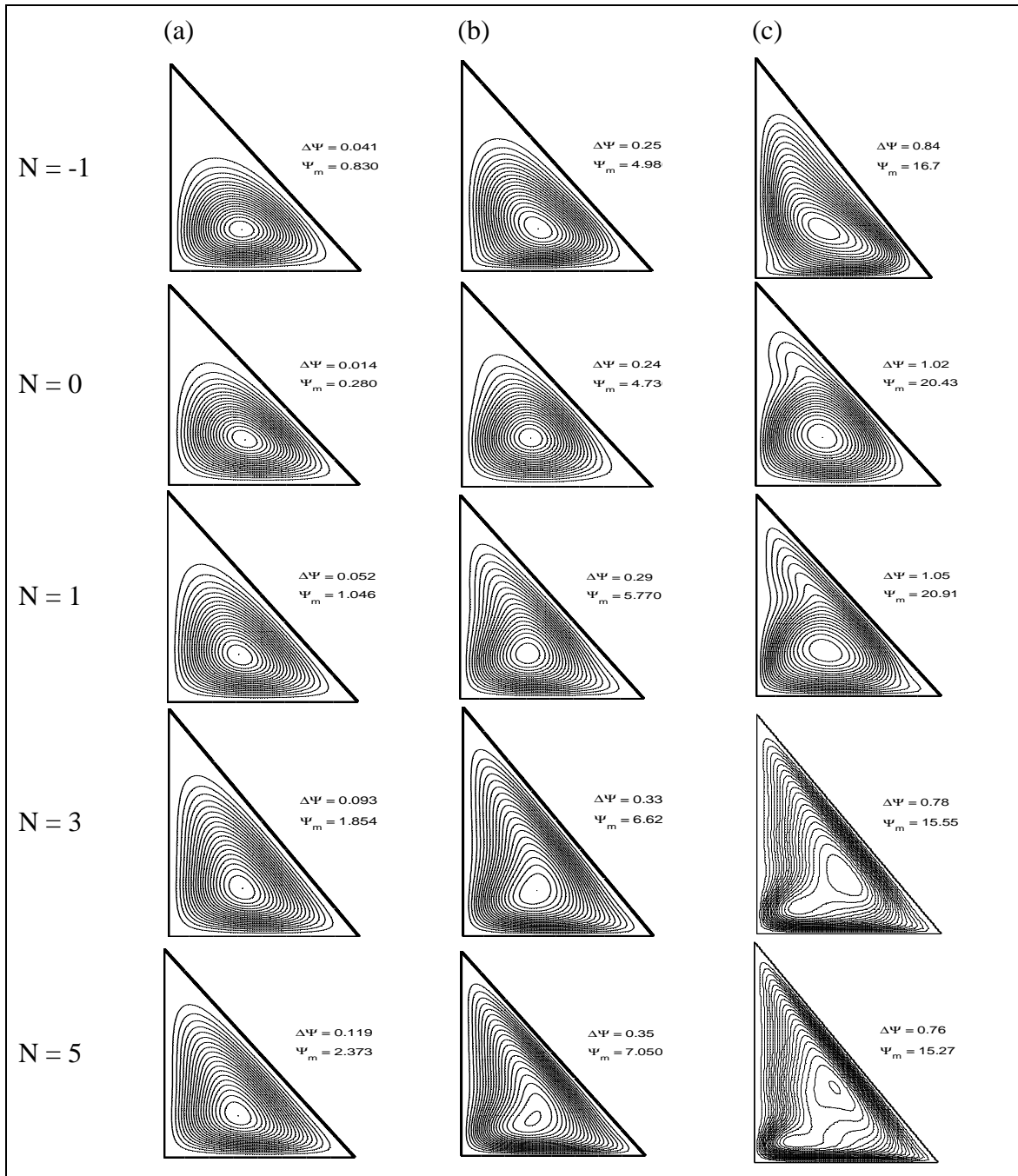


Fig. 10. Effect of Buoyancy Ratio on Streamlines at Le=2, and $\theta = 60^\circ$ for (a) Ra=10³, (b) Ra=10⁴, and (c) Ra=10⁵.

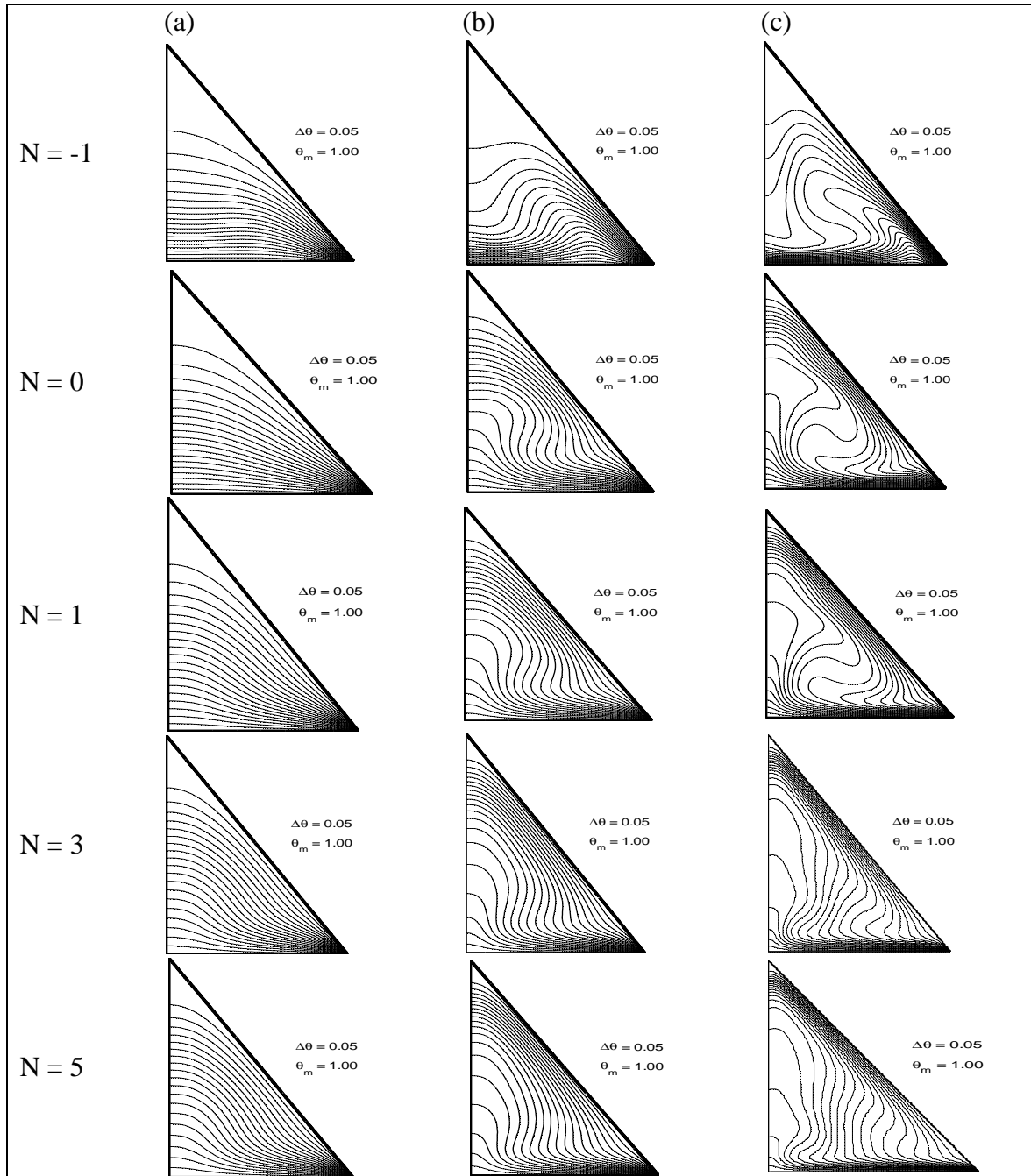


Fig. 11 .Effect of Buoyancy Ratio on Isotherms at $Le=2$, and $\phi = 60^\circ$ for (a) $Ra=10^3$, (b) $Ra=10^4$, and (c) $Ra=10^5$.

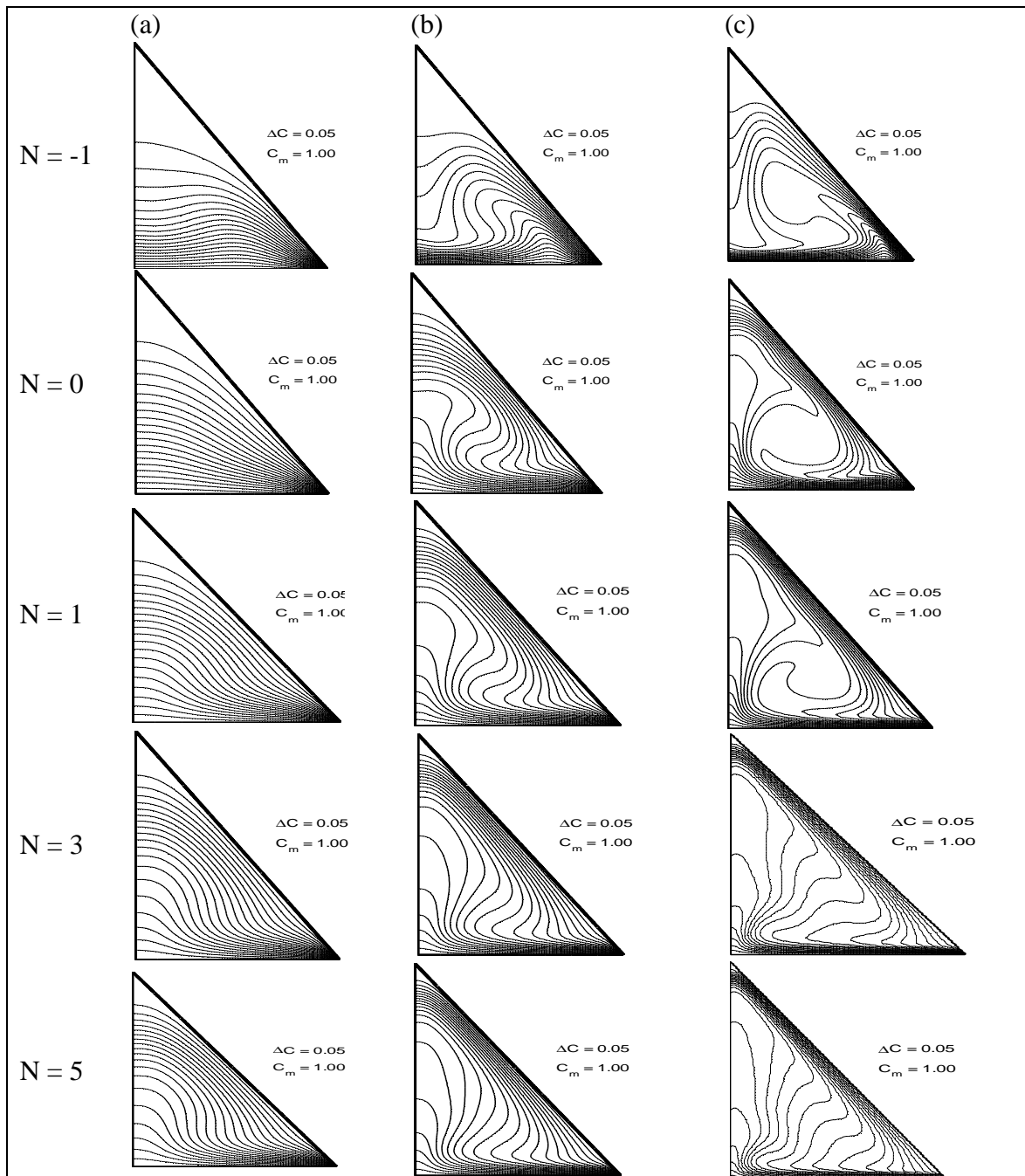


Fig. 12. Effect of Buoyancy Ratio on Isoconcentration at $Le=2$, and $\theta = 60^\circ$ for (a) $Ra=10^3$, (b) $Ra=10^4$, and (c) $Ra=10^5$.

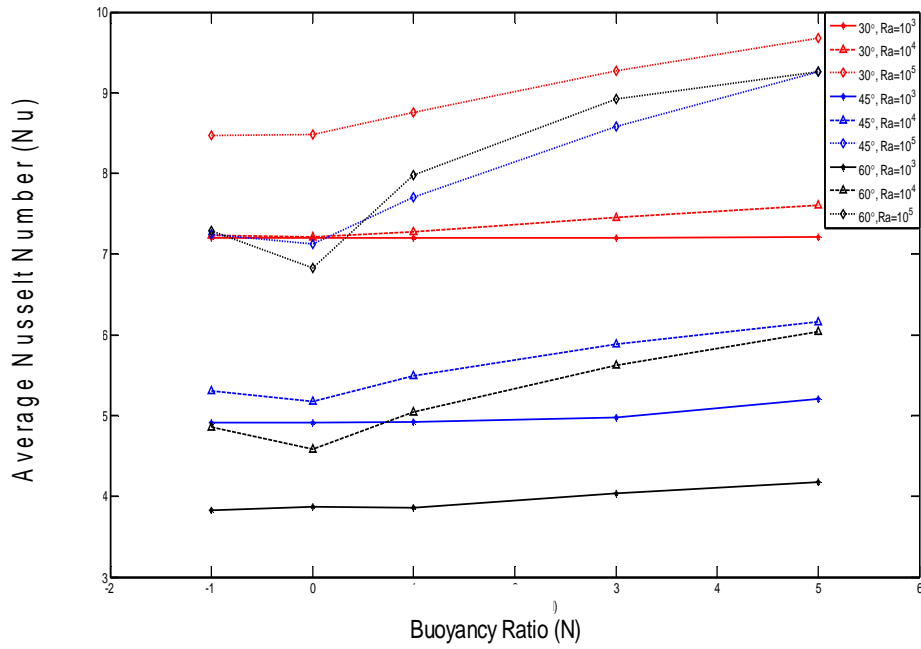


Fig. 13. Effect of Buoyancy Ratio at Different (Ra) and Different (θ), on Average Nusselt Number.

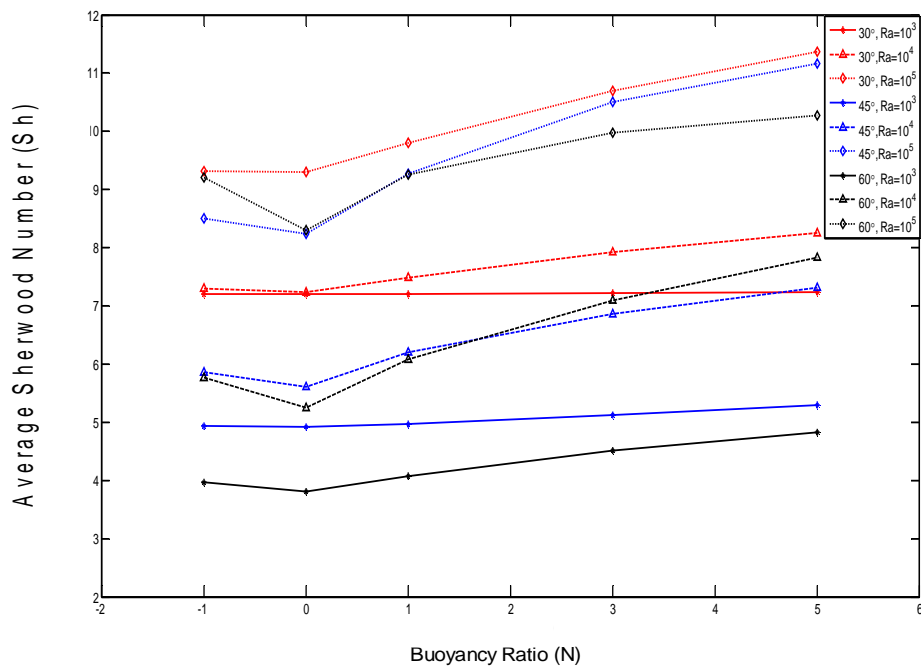


Fig. 14. Effect of Buoyancy Ratio at Different (Ra) and Different (θ), on Average Sherwood Number.

4. Results and Discussion

Numerical analysis of double diffusive laminar natural convection in a right triangular solar collector has been made in current work for different Rayleigh numbers Ra (10^3 - 10^5), Buoyancy ratio N (-1 - 5), and angle of inclined glass cover with horizontal coordinate θ (30° - 60°) via finite difference technique. The working fluid inside the cavity was the air, with $Pr=0.71$, and the Lewis number was held fixed through this investigation at ($Le = 2$). The numerical results in form of the streamlines, isotherms, isoconcentration, average Nusselt, and average Sherwood number numbers for various values of the parameters governing the heat transfer and fluid flow will be presented and discussed. Indeed, for ($-1 \leq N < 0$) The thermal buoyancy force due to the heat transfer and thermal expansion, (which acts to the upward direction) opposes the buoyancy force due to the mass transfer, (which acts to the downward direction). As a result, there is a very weak flow due to competition between two forces. The fluid moves downward from the upper summit and the flow transforms on one small cell turning from the center to the cold sides brushing against the bottom vicinities. For positive buoyancy ratios ($N > 0$), the heated flow moves from bottom wall and impinges to the inclined wall and one cell formed in clockwise direction. Figures (4,7,10) illustrates the effect of buoyancy ratios on streamlines at different (Ra) and different (θ). As Rayleigh numbers or buoyancy ratios increases, the rotating cell occupies more space inside the cavity, indicating that the convection currents become more effective and that heat transfer by convection become more predominate. The maximum stream function value is obtained for $N = 5$, $Ra=10^5$, and ($\theta = 60^\circ$). Fig (5,8,11) illustrates the isotherms contours at different Rayleigh numbers and different buoyancy ratios. One can observe that the patterns of the isotherms contours are related to the buoyancy ratio values and Rayleigh numbers. Obviously, the convection effects are more effective at the positive buoyancy ratios. It should also be noted that when the buoyancy ratios or Rayleigh numbers increases, the temperature field develops quickly. In comparison, for negative buoyancy ratios values, one can observe a kind of stratification indicating the conductive regime domination. Isoconcentration contours at different Rayleigh numbers and different buoyancy ratios are illustrates in Figures (6,9,12). Distribution of

isoconcentration contours reveal a similar distribution with distribution of isotherm contours. Both Rayleigh numbers and buoyancy ratio have a strong influence on the streamlines patterns, isotherms, isoconcentration, and enhance the flow strength. Figures (13,14) illustrates the effect of increase in Rayleigh numbers and angle of inclined glass cover with horizontal coordinate at different buoyancy ratios on the average Nusselt number and average Sherwood number, respectively. For negative buoyancy ratios the values for average Nusselt number and average Sherwood number decreases. By contrast, for positive buoyancy ratios, the values for average Nusselt number and average Sherwood number increases when the Rayleigh numbers and buoyancy ratios increases.

5. Conclusions

The results of the present study lead to the following conclusions:

- The results show that both Rayleigh number and buoyancy ratio have a strong effect on the streamline patterns, isotherms, and isoconcentration.
- Results show that a decrease in the angle of inclined glass cover with horizontal coordinate (θ) leads to increase average Nusselt number and average Sherwood number.
- For ($N > 0$), both average Nusselt number and average Sherwood number increase with increasing of buoyancy ratio and Rayleigh number. By contrast for ($N < 0$) these values decreases. Also, increasing of the buoyancy ratio for positive values ($N > 0$), at the same Rayleigh number enhance the heat and mass transfer rate.

Nomenclature

H	Solar collector height (m)
L	Solar collector length (m)
N	Buoyancy ratio
c	Dimensional species concentration
C	Dimensionless species concentration
D	Species diffusivity ($m^2 kg^{-2} s^{-1}$)
g	Gravitational acceleration ($m s^{-2}$)
Le	Lewis number
Nu	Average Nusselt number
p	Dimensional pressure

P	Dimensionless pressure
Pr	Prandtl number
Ra	Rayleigh number
Sh	Average Sherwood number
T	Wall temperature (K)
u, v	Dimensional velocity components ($m s^{-1}$)
U, V	Dimensionless velocity components
x, y	Dimensional coordinates (m)
X, Y	Dimensionless coordinates

Greek symbols

α	Thermal diffusivity ($m^2 s^{-1}$)
β	Expansion coefficient (K^{-1})
ν	kinematic viscosity ($m^2 s^{-1}$)
θ	Dimensionless temperature
ρ	Density ($kg m^{-3}$)
ω	Dimensional vorticity
Ω	Dimensionless vorticity
ψ	Dimensional stream function
Ψ	Dimensionless stream-function
Δ	Laplacian in Cartesian coordinates
θ	Angle of inclined glass cover with horizontal coordinate

Superscripts

ζ	Current iteration number
$\zeta-1$	Previous iteration number

Subscripts

h	High
l	Low
H	Hot
L	Cold
T	Thermal
C	C
∞	Fluid at the bottom surfaces

References

- [1] Hitesh N Panchal, Dr. P. K. Shah, [Effect of varying glass cover thickness on performance of solar still in winter climate conditions], International Journal of Renewable Energy Research, Vol.1, No.4 (2011) 212-223.
- [2] Hiroshi Tanaka, [A theoretical analysis of basin type solar still with flat plate external reflector], Desalination 279 (2011) 243-251.
- [3] Narjes Setoodeh, Rahbar Rahimi, Abolhasan Ameri, [Modeling and determination of heat transfer coefficient in a basin solar still using CFD], Desalination 268 (2011) 103-110.
- [4] M.M. Rahman, Hakan F. Oztop, A. Ahsan, M.A. Kalam, Y.Varol, [Double diffusive natural convection in a solar collector], International Communications in Heat and Mass Transfer 39 (2012) 264-269.
- [5] Mohamed A. Teamah, [Numerical simulation of double diffusive natural convection in rectangular enclosure in the presences of magnetic field and heat source], International Journal of Thermal Sciences 47 (2008) 237-248.
- [6] Ching-Yang Cheng, [Double diffusive natural convection along an inclined wavy surface in a porous medium], International Communications in Heat and Mass Transfer 37 (2010) 1471-1476.
- [7] Ching-Yang Cheng, [Combined heat and mass transfer in natural convection flow from a vertical wavy surface in a power-law fluid saturated porous medium with thermal and mass stratification], International Communications in Heat and Mass Transfer 36 (2009) 351-356.
- [8] Yasin Varol, Hakan F. Oztop, Asaf Varol, [Free convection in porous media filled right-angle triangular enclosures], International Communications in Heat and Mass Transfer 33 (2006) 1190-1197.
- [9] [9] Ali J. Chamkha, Hameed Al-Naser, [Hydromagnetic double diffusive convection in a rectangular enclosure with opposing temperature and concentration gradients], International Journal of Heat and Mass Transfer 45 (2002) 2465-2483.
- [10] E. Fuad Kent, E. Asmaz, S. Ozerbay, [Laminar natural convection in right triangular enclosures], Heat Mass Transfer (2007) 44: 187-200.
- [11] E. F. Kent, [Numerical analysis of laminar natural convection in isosceles triangular enclosures], DOI: 10.1243/09544062JSME1122 (2008).
- [12] Yoshio Masuda, Michio Yoneya, and Shin-ichi Sumi, [Double-Diffusive Natural Convection in a Porous Medium under Constant Heat and Mass Fluxes], Heat Transfer—Asian Research, Vol. 28 (1999), 255–265.
- [13] Mohamed A. Teamah, [Double-diffusive laminar natural convection in a symmetrical trapezoidal enclosure], Alexandria Engineering Journal, Vol. 45, (2006), No. 3, 251-263.

دراسة عددية للحمل الحر الطبقي ثنائي الانتشار في مجمع شمسي مثلث قائم الزاوية

جاسم محمد مهدي* علي محسن رشم** ثامر حارث علي***

***،** قسم هندسة الطاقة / كلية الهندسة / جامعة بغداد

** كلية الهندسة الخوارزمي / جامعة بغداد

* البريد الإلكتروني: jasim_ned@yahoo.com

** البريد الإلكتروني: ali_mohsen7788@yahoo.com

*** البريد الإلكتروني: thamir.2008@yahoo.com

الخلاصة

يُقدم البحث الحالي دراسة عددية للحمل الحر الطبقي ثنائي الانتشار في مجمع شمسي مثلث قائم الزاوية. وقد فُرضَ ثبات درجة الحرارة والتركيز لكل من ارضية المجمع والسقف الزجاجي. بينما الجدار العمودي اعتُبرَ معزول حرارياً وغير نفاذ. وقد تم دراسة اتحاد وتضاد اتجاه قوى الطفو. المعادلات الحاكمة مُثلت بصيغة الدوامية -دالة الجريان و تم تحويلها إلى صورة لا بعدية مناسبة و قد تم استخدام طريقة الفروقات المحددة تُحل عددياً بأسلوب الإرخاء. وتم صياغة برنامج حاسوبي خاص ضمن برنامج الماتلاب لتنفيذ وحل النموذج الرياضي في هذه الدراسة. لقد مُثلت النتائج بشكل خطوط السريان وخطوط ثبات الحرارة وخطوط ثبات التركيز ورقم نسلت وشيروود المتوسط، و لمدى واسع للنسبة بين قوتي الطفو من (١- إلى ٥) وزاوية ميل الغطاء الزجاجي من (٣٠ - ٦٠ درجة) و (رقم لويس = ٢) ورقم رايلي الحراري من (١٠^٢ - ١٠^٥) و (رقم برانتل = ٠,٧١). وتم دراسة تأثير النسبة بين قوتي الطفو ورقم رايلي الحراري وزاوية ميل المجمع على خطوط السريان وخطوط ثبات الحرارة وخطوط ثبات التركيز وعلى كل من رقم نسلت ورقم شيروود المتوسط. وقد أظهرت النتائج بأن العوامل اعلاه لها تأثير قوي على تشكيل نماذج خطوط السريان وخطوط ثبات الحرارة وخطوط ثبات التركيز وكذلك رقم نسلت ورقم شيروود المتوسط. اظهرت النتائج زيادة في رقم نسلت المتوسط ورقم شيروود المتوسط عند نقصان زوايا ميل المجمع. إضافة الى ذلك، بزيادة نسبة الطفو ($N > 0$) ورقم رايلي الحراري يزداد رقم نسلت المتوسط ورقم شيروود المتوسط وبالعكس لنسب الطفو ($N < 0$). وكذلك ان الزيادة في نسب قوى الطفو ($N > 0$) ولرقم رايلي حراري واحد يُحسن معدل انتقال الحرارة والكتلة. وقد تم المقارنة مع نتائج ابحاث السابقة وقد اظهرت النتائج توافق جيد مع الابحاث المنشورة.